RADIATION RESEARCH **174**, 357–366 (2010)
0033-7587/10 $15.00

DOI: 10.1667/RR2143.1

The Balance Between Initiation and Promotion in Radiation-Induced Murine Carcinogenesis

Igor Shuryak,[a] Robert L. Ullrich,[b] Rainer K. Sachs[c] and David J. Brenner[a,1]

[a] *Center for Radiological Research, Columbia University Medical Center, New York, New York;* [b] *Department of Radiation Oncology, The University of Texas Medical Branch, Galveston, Texas; and* [c] *Departments of Mathematics and Physics, University of California Berkeley, California*

Shuryak, I., Ullrich, R. L., Sachs, R. K. and Brenner, D. J. The Balance between Initiation and Promotion in Radiation-Induced Murine Carcinogenesis. *Radiat. Res.* 174, 357–366 (2010).

Studies of radiation carcinogenesis in animals allow detailed investigation of how the risk depends on age at exposure and time since exposure and of the mechanisms that determine this risk, e.g., induction of new pre-malignant cells (initiation) and enhanced proliferation of already existing pre-malignant cells (promotion). To assist the interpretation of these patterns, we apply a newly developed biologically based mathematical model to data on several types of solid tumors induced by acute whole-body radiation in mice. The model includes both initiation and promotion and analyzes pre-malignant cell dynamics on two different time scales: comparatively short-term during irradiation and long-term during the entire life span. Our results suggest general mechanistic similarities between radiation carcinogenesis in mice and in human atomic bomb survivors. The excess relative risk (ERR) in mice decreases with age at exposure up to an exposure age of 1 year, which corresponds to mid-adulthood in humans; the pattern for older ages at exposure, for which there is some evidence of increasing ERRs in atomic bomb survivors, cannot be evaluated using the data set analyzed here. Also similar to findings in humans, initiation dominates the ERR at young ages in mice, when there are few background pre-malignant cells, and promotion becomes important at older ages.

INTRODUCTION

Most mathematical models of spontaneous and radiation-induced carcinogenesis either emphasize comparatively short-term processes and make simplistic assumptions about long-term ones [e.g. refs. (*1–5*)] or vice versa [e.g. refs. (*6–15*)]. In two previous articles (*16, 17*) we presented a new model that integrates relatively detailed analyses of those processes that operate during or shortly after irradiation (i.e. cell *i*nitiation, *i*nactivation and *r*epopulation, abbreviated as *iir*) with analyzing processes that operate on typically longer time scales before and after exposure (e.g., the growth kinetics of stem cell niches filled with pre-malignant initiated cells). The assumptions for the short- and long-term parts of the formalism are similar to those used in other models [specifically in the stochastic *iir* model (*2*) and a deterministic version of the two-stage clonal expansion model (*18*), respectively], so the combined model can generally describe the short- and long-term data as well as these other formalisms (*16, 17*). The advantage of a unified approach is that interactions between short- and long-term processes, such as modulation of the shape and magnitude of the initial dose response over the long period after radiation exposure before cancer development, are analyzed directly and in more detail than would be possible using short- or long-term models alone.

We previously applied our model to the task of predicting radiotherapy-induced cancers, using second cancer data for nine solid cancer types—stomach, lung, colon, rectal, pancreatic, bladder, breast, CNS and thyroid—in patients treated by radiotherapy for various primary cancers (*17*). Some of the model parameters were obtained from fitting radiogenic risks at comparatively low doses for Japanese atomic bomb survivors or from background U.S. cancer incidence data. The focus was on the shape of the radiation dose response at high fractionated radiation doses typical for cancer radiotherapy. Here we apply the same model to radiation-induced tumors in mice with an emphasis not as much on the dose response but on the dependences of the cancer risk on age at exposure and time since exposure and on the underlying mechanisms that determine this risk. The specific mouse data sets (described below) selected for this analysis are particularly well suited for investigating the patterns of such dependences due to the experimental design used to generate them. Understanding these patterns within the context of a biologically based mathematical model is potentially useful because

[1] Address for correspondence: Center for Radiological Research, Columbia University Medical Center, 630 West 168th St., New York, NY 10032; e-mail: djb3@columbia.edu.

TABLE 1
Summary of Model Parameters

	Units	Interpretation	Restrictions
a	time^{-2}	Spontaneous stem cell initiation and transformation	none
b	time^{-1}	Pre-malignant niche replication	none
c	time^{-2}	Pre-malignant cell aging	none
δ	time^{-1}	Homeostatic regulation of pre-malignant cell number per niche	none
Z	cells/niche	Carrying capacity for pre-malignant cells per niche	$Z = 1$
X	time/dose	Radiation-induced initiation	none
Y	dose^{-1}	Radiation-induced promotion	none
α, β	dose^{-1}, dose^{-2}	Stem cell inactivation by radiation	$0.2 < \alpha < 0.6$ Gy^{-1}; $\beta = 0$
L	time	Lag period between the first fully malignant cell and cancer	$L = 100$ days for cancer incidence, 200 for mortality

it can shed some light on the individual contributions of different carcinogenic mechanisms to the overall cancer risk (*6–10, 19, 20*).

These mechanisms can be grouped into two general categories: (1) induction of alterations such as mutations in normal stem cells, either spontaneously or by radiation, which shifts the altered cells into a pre-malignant state, with the potential of becoming fully malignant upon acquiring additional alterations, and (2) radiation-induced increases in the number of already existing pre-malignant cells, for example due to acceleration of their proliferation. The first process is usually labeled *initiation*, and the second *promotion*. As we discuss below, the contributions of each of these mechanisms to radiogenic cancer risk can have quite different dependences on age at exposure and on other relevant variables. We believe that the insight about these phenomena gained by analyzing animal data can subsequently be used, at least conceptually or qualitatively, to better understand the mechanisms of radiation carcinogenesis in humans.

METHODS

Model Used

The detailed assumptions and mathematical implementation of our model were described elsewhere (*16*). Briefly, the model assumes that normal organ-specific stem cells, which reside in stem cell niches or compartments, referred to generically as "niches", can be initiated to a pre-malignant state, either spontaneously or by radiation, and can then be transformed into fully malignant cells, which form tumors after some lag time. The parameters needed to apply this formalism to the selected data sets (discussed below), where a single acute radiation dose was administered, are presented in Table 1. To reduce the number of adjustable constants, we restricted some parameters to biologically plausible values or ranges (Table 1).

The equation for the mean expected number of new fully malignant cells per individual per unit time under background conditions (A_{bac}, units = time^{-1}), which is an approximation for the cancer hazard function L time units later, was derived previously (*16, 17*). It is repeated below, using the notation where age is defined as the sum of age at exposure (T_x) and the time after exposure (T_y):

$$A_{bac} = (a/b)\left(\exp\left[b\left(T_x + T_y\right)\right] - 1\right)\exp\left[-c\left(T_x + T_y\right)^2\right]. \quad (1)$$

The expression for [1]the radiation-induced excess relative risk (ERR) after a single acute radiation dose D is:

$$\begin{aligned} &\mathrm{ERR} = [(\mathrm{Q}_1\mathrm{Q}_2 + \mathrm{Q}_3)/\mathrm{Q}_4] - 1, \text{ where :} \\ &\quad \mathrm{Q}_1 = (1 + Y\,D)/\left[1 + Y\,D\left(1 - \exp\left[-\delta\,T_y\right]\right)\right]; \\ &\quad \mathrm{Q}_2 = \left[\left(\exp[b\,T_x] - 1\right)\left(1 - \left(1 - \exp\left[-\alpha\,D - \beta\,D^2\right]\right)^Z\right)\right. \\ &\qquad \left. + b\,X\left(D\exp\left[-\alpha\,D - \beta\,D^2\right]\right)\right]\exp\left[b\,T_y\right]; \\ &\quad \mathrm{Q}_3 = \exp\left[b\,T_y\right] - 1;\ \mathrm{Q}_4 = \exp\left[b\left(T_x + T_y\right)\right] - 1. \end{aligned} \quad (2)$$

Data Sets and Model Fitting Procedure

The data used in this analysis were derived from two papers by Sasaki and Fukuda (*21, 22*) on the incidence of and mortality from several tumor types in female B6C3F1 mice exposed to acute doses of γ rays. These specific studies were chosen because they measured tumor incidence not only at several radiation doses but also at several ages at exposure and times after exposure, so that relatively detailed information on the temporal trends of the risk is available. As noted previously, investigating and interpreting these trends within the context of our model is the main aim of this paper.

Fitting of the model (Eqs. 1 and 2) to the data was carried out using a customized random-restart simulated annealing algorithm implemented in FORTRAN. First, the best-fit values of those parameters that determine background tumor risk (i.e. a, b, c) were generated for the age- and time-dependent mortality from all solid tumors combined in unirradiated mice. This was done because the data for this lumped category were more detailed and statistically robust than those for individual tumor types. Second, the model was fitted to the ERRs at various doses, ages at exposure and times since exposure for (1) mortality from all solid tumors combined and (2) incidences of four specific tumor types—bone, liver, lung and pituitary. These organs were chosen because they presumably do not undergo dramatic modulation by sex-related hormones, and so the simplistic model assumptions, which do not account for hormones, may be more applicable. In contrast, ovarian carcinogenesis is probably strongly affected by hormones and may exhibit a complex dose response where some degree of oocyte killing is necessary for carcinogenesis [e.g. ref. (*23*)]. Also, the four selected tumor types were more common in the mouse strain used by Sasaki and Fukuda than some other neoplasms (e.g. renal, harderian gland), so the data on these types were more robust. Only the data for exposures after birth were used, setting the time of birth as age zero. Data for the *in utero* period, which have a very different behavior, were not included because analyzing them may require more

TABLE 2
Best-Fit Parameter Values (and 95% Confidence Intervals) for all Analyzed Tumor Types

Tumor type	Data	$10^8 \times a$ day^{-2}	$10^2 \times b$ day^{-1}	$10^6 \times c$ day^{-2}	L day
All solid tumors	Mortality	1.42 (0.9, 2.1)	1.59 (1.2, 2.1)	6.54 (4.5, 8.5)	200
Bone	Incidence	–	1.59 (0.6, 2.2)	–	100
Liver	Incidence	–	1.59 (1.1, 2.3)	–	100
Lung	Incidence	–	1.59 (1.1, 2.7)	–	100
Pituitary	Incidence	–	1.59 (1.1, 2.5)	–	100

Tumor type	$10^4 \times \delta$ day^{-1}	X day $\times$ Gy^{-1}	Y Gy^{-1}	X/Y days	α Gy^{-1}
All solid tumors	2.11 (0.2, 3.9)	79.7 (20, 250)	12.2 (0.1, 170)	6.5	0.60 (0.3, 1.1)
Bone	2.11 (0.5, 7.6)	79.7 (22, 340)	1.99 (0.2, 15)	40	0.20 (0.1, 0.5)
Liver	2.11 (0.2, 12)	79.7 (53, 160)	0.596 (0.3, 4.6)	130	0.273 (0.1, 0.6)
Lung	2.11 (0.5, 5.5)	79.7 (5.0, 950)	1.77 (0.1, 25)	45	0.60 (0.4, 0.9)
Pituitary	2.11 (0.3, 8.4)	79.7 (56, 130)	0.459 (0.2, 2.6)	170	0.283 (0.0, 0.8)

Notes. Parameter interpretations and restrictions are listed in Table 1. The ratio X/Y is shown for easier comparison of initiation/promotion balance between different cancer sites; it is not a model parameter.

complicated model assumptions. This issue is discussed below in more detail.

Because of the structure of our model, the parameters a and c cancel out of the ERR expression (Eq. 2). Consequently, only five adjustable parameters (b, δ, X, Y and α) are needed to describe the ERR for either cancer incidence or mortality. To further reduce this number, we attempted to keep the values of as many parameters as possible in common across tumor types rather than allowing them to attain specific values for each type. Exploratory calculations suggested that reasonable fits for all the data could be generated by keeping in common the values of the parameters for pre-malignant niche replication (b), estimated from fitting the background mortality data for all tumors combined, and radiation-induced initiation (X) and homeostatic regulation of the number of pre-malignant stem cells per niche (δ), both estimated from fitting the ERRs for mortality from all solid tumors combined and incidences of individual tumor types. The number of tumor-specific adjustable parameters needed to fit the ERR data for any individual tumor type was therefore reduced to only two: the radiation-induced promotion constant (Y) and the cell killing constant (α).

Clearly the approach of selecting cross-tumor parameters based on fitting results is imperfect. Improved estimates of all of these parameters may become possible in the future due to advances in experimental studies of mouse carcinogenesis. The main goal of the current procedure was to reduce the number of parameters, so that the results could be interpreted more easily and potential mechanistic patterns identified. Reducing the parameter space is also beneficial because it increases the probability of finding the global rather than a local minimum. This probability was enhanced by running the fitting algorithm several times using different random number initiation "seeds" and monitoring the deviance as a function of number of iterations. The obtained best-fit parameter combination was deemed to be the global minimum because the algorithm converged on it regardless of the initial random number and regardless of increases in the number of iterations beyond a certain value.

For all tumor types the model-predicted ERRs were estimated for attained ages that corresponded to the mean survival ages of the mice in each experimental group, which approximated lifetime ERR. As the radiation dose increased, the mean survival age decreased, as expected. Hence the effects of both age at exposure and time since exposure, the sum of which comprises attained age, were accounted for.

Ninety-five percent confidence intervals for all adjustable parameters were estimated by generating multiple synthetic data sets based on the experimental data set and fitting the model to these synthetic data sets. The simulated data sets were produced using the data points and standard errors reported by Sasaki and Fukuda (*21, 22*), assuming the normal distribution.

RESULTS

The best-fit model parameters for mortality from all solid tumors and for incidences of bone, liver, lung and pituitary tumors are listed in Table 2. The analyzed data can be adequately described even with multiple restrictions on model flexibility, such as keeping several parameter values in common for all tumor types and restricting some others to biologically plausible ranges or values. A possible interpretation of these findings is that in the studied mouse strain the net replication rate for niches filled with pre-malignant cells (b) may be similar regardless of the organ in which these pre-malignant cells are found, and the same can be said about the homeostatic regulation of the number of cells per niche (δ) and about the dose-dependent ability of radiation to initiate new pre-malignant cells (X) relative to the spontaneous initiation rate for each tumor type. The major differences between the mouse tumor types may therefore be attributable to differences in radiogenic promotion (Y) and cell killing (α). The ratio between the initiation and promotion parameters (X/Y) varies considerably between cancer types, suggesting that in these mice promotional mechanisms may be much more important for some cancers than for others.

This scheme may be plausible to some extent, for example because (1) radiogenic promotion is interpreted in the context of our model as deregulation of cell-cell signals that maintain stem cell niche sizes, (2) cell-cell signals can be modulated by radiation-induced oxidative stress and other processes [e.g. refs. (*24–26*)], and (3) the magnitude and nature of the modulation may be organ/cell type-dependent. Consequently, radiogenic promotion may be more organ-specific than initiation. Differences in radiosensitivity (α) between stem cells from different mouse organs are also likely, for example

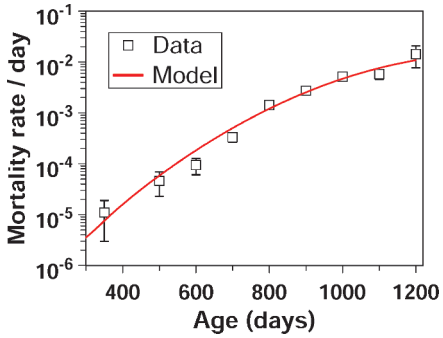

FIG. 1. The data and best-fit model predictions for the background mortality rate from all solid tumors combined. The data in this figure and the following figures are from refs. (*21, 22*). In this and the following figures, error bars represent standard errors.

because the stem cells in rapidly renewing tissues may be much more mitotically active, and hence more radiosensitive, than stem cells in tissues where cell turnover is slower; e.g. hematopoietic stem/progenitor cells are more radiosensitive (*27*) than breast stem cells (*28*).

The estimates of 95% confidence intervals for the adjustable parameters are also provided in Table 2. Notably, these estimates can be quite asymmetric around the best-fit values. This is due in part to the fact that the best-fit values for some parameters (δ, X, b) were determined by analyzing all tumor types together rather than individually. Consequently, the best-fit values listed for a given tumor type do not represent the optimal combination for that particular tumor type (which would be based on a deviance minimum for that type alone) but were obtained by optimizing the total deviance for a larger data set that includes information on other tumors. The confidence intervals, however, apply specifically to each selected tumor type, to provide a sense of how the fit for each type is affected by altering the default parameter values.

The greatest model sensitivity, represented by the tightest confidence intervals, occurred for the premalignant niche replication rate b because this parameter strongly affects both the background risk and the radiation-induced risk (see Eqs. 1, 2). The model was also relatively sensitive to the value of the cell killing constant α, because this constant has a substantial effect on the shape of the radiation dose response. Sensitivity to other parameters was generally less pronounced. For example, confidence intervals for the radiation initiation constant X were often very wide (Table 2), which is consistent with the fact that this parameter could be kept in common across tumor types without altering the fit dramatically. These results suggest that the formalism can adequately fit the selected data sets using many possible parameter value combinations, so that conclusions based on specific parameter values should be interpreted cautiously without additional information about these values, e.g. from other experimental data.

The model fit to the age-dependent mortality rate from all solid tumors in unirradiated mice is shown in Fig 1. Figure 2 shows the data and best-fit model predictions for the ERR for mortality from all solid tumors at a dose of 1.9 Gy as function of age at exposure and time since exposure. Generally, the model describes the data reasonably, considering the uncertainties in the data points. The decreasing trend in the ERR with time since exposure is well accounted for.

There is, however, some qualitative discrepancy between the data and predictions for the effects of age at exposure: The model predicts a monotonic decrease in ERR with age at exposure for a fixed attained age (some effect of attained age is also seen because of progressive life shortening at increasing radiation doses, but this effect is not dominant in the data analyzed here). The mouse data, however, suggest that ERR actually grows during the late *in utero* period (not included in the analysis here) and the first days of life and begins to decrease only after 35 days. A similar pattern has recently been observed in humans using data from Japanese atomic bomb survivors (*29*). A possible interpretation is that the ERR is affected by the physiological processes during active organ growth, which occur *in utero* and during the neonatal period both in mice and in humans, e.g. changes in the number and/or the radiosensitivity of stem cells available for oncogenic transformation, and/or more efficient elimination of pre-malignant cells by cell-cell interactions. The model in its current form does not account for these processes and assumes that the target cell numbers and dynamics are the same regardless of age; such assumptions were made for simplicity.

Figure 3 shows the data and best-fit model predictions for the ERR for incidence of specific tumor types as a function of age at exposure (estimated for an attained age corresponding to the mean survival age for each experimental group) for mice irradiated with 1.9 Gy. For these tumor types, the data support a relatively monotonic decrease in ERR with age at exposure to a better extent than the data for all solid tumors combined referred to earlier. For this reason, qualitative agreement with model predictions is better as well. The explanation for a decrease of the ERR with age at exposure within the context of our model has been described in detail in previous papers (*16, 17*). If excess risk is dominated by radiation initiation rather than radiation promotion, it occurs mainly for the following reasons: (1) cells initiated at an early age have longer to exploit their growth advantage over normal cells (if the attained age of maximal cancer incidence is relatively constant); (2) cellular proliferation rates early in life can be more rapid, making target cells more sensitive to radiogenic initiation. The number of "background" premalignant cells increases with age, increasing the cell population on which promotional processes can act but

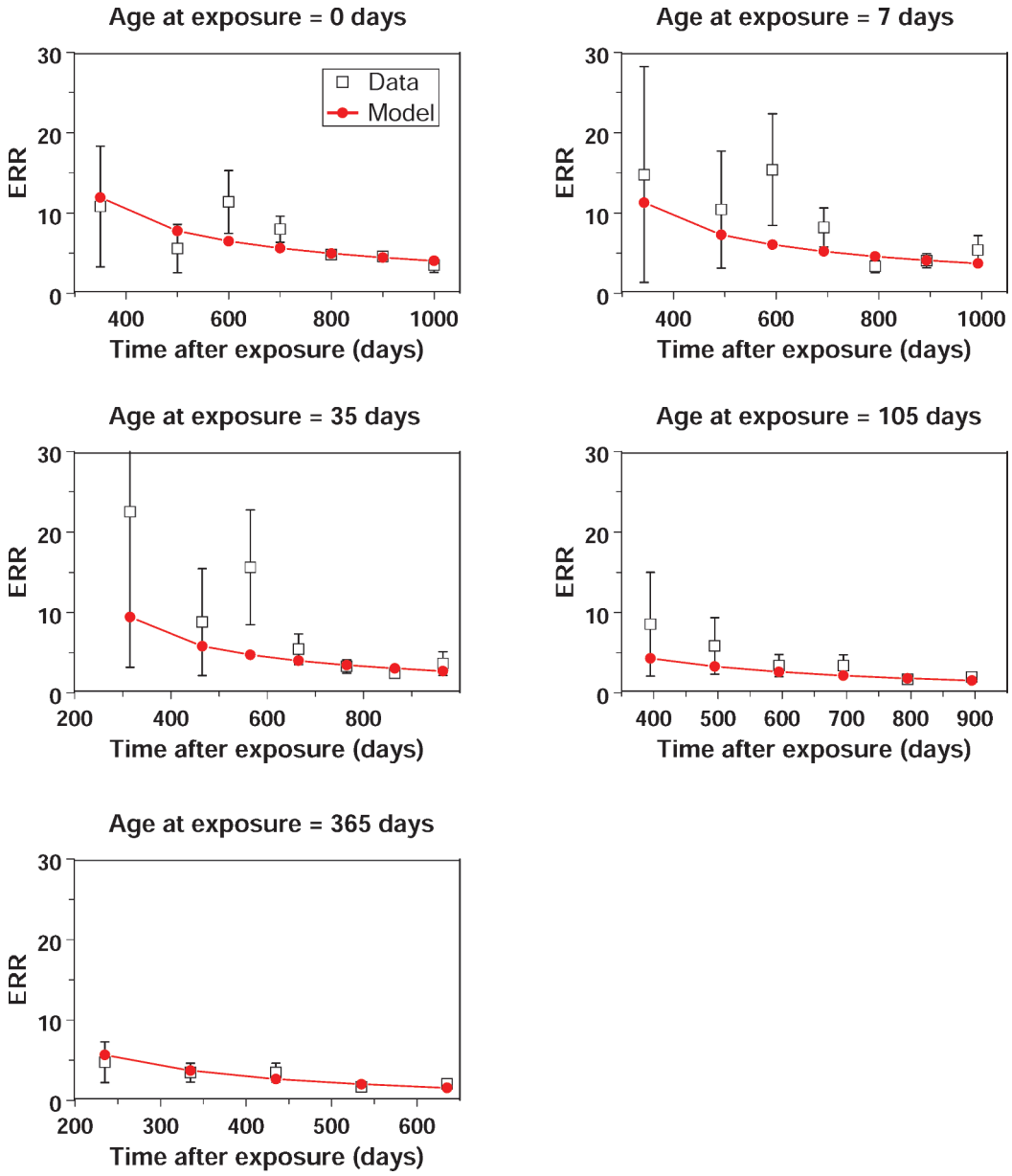

FIG. 2. The data and best-fit model predictions for the excess relative risk (ERR) for mortality from all solid tumors combined at a dose of 1.9 Gy. In this and the following two figures, the model predictions corresponding to the data points are represented by points (filled circles), which were generated using the corresponding combinations of dose, age at exposure, and time since exposure. The lines connecting the predicted points are shown for convenience only.

decreasing the fractional contribution of initiated cells to total cancer risk by increasing the denominator of the ERR. When irradiation occurs at a young age, there are few existing pre-malignant cells, so promotion of these cells (i.e. multiplicative amplification of their number) is a small effect compared with the much larger number of new pre-malignant cells created by radiation. For irradiation at a much older age, the reverse is true: there are many already existing pre-malignant cells compared with the number of new cells initiated by radiation, and promotion of the existing large pre-malignant cell population becomes much more important.

The radiation dose responses for the selected tumor types are shown in Fig. 4. The structure of Eq. (2) produces a dose–response shape that is essentially linear at low doses and then peaks and turns over at higher doses due to cell killing. This generic shape describes the data reasonably well, particularly for mouse liver and pituitary tumors, among those analyzed here. For mouse lung tumors, the model underestimates the slope of the dose response at low doses and the rate of decline at high doses. The predicted decline at high doses is determined by the cell killing constant α and could be enhanced by allowing the value of this parameter to be >0.6 Gy^{-1}

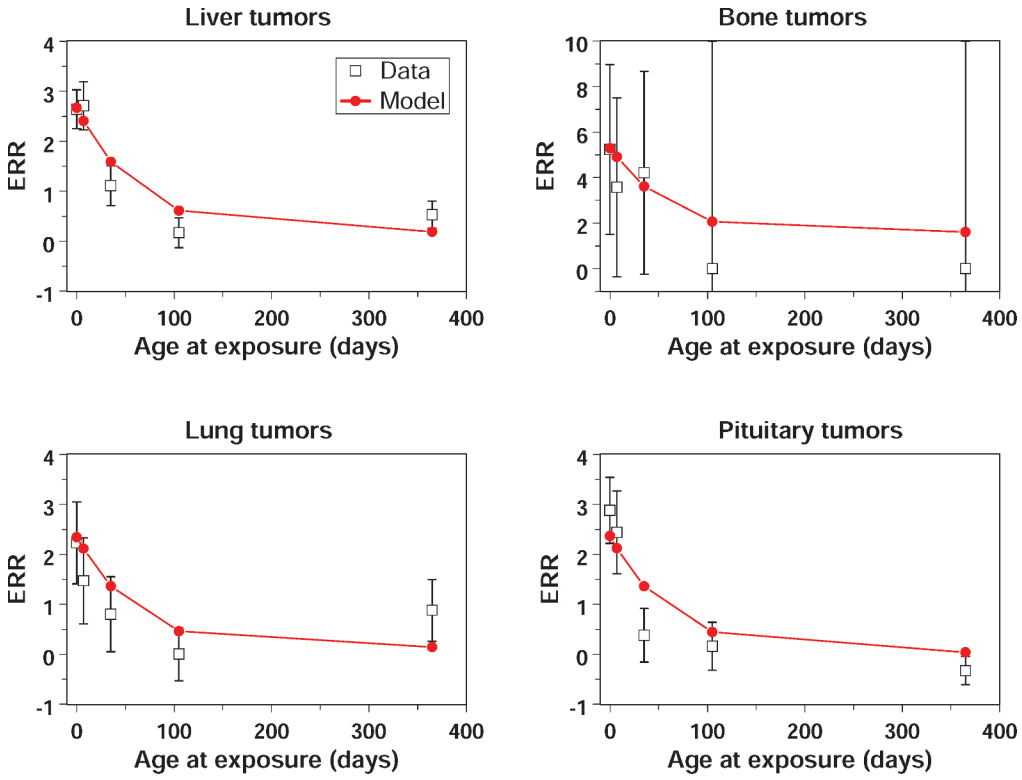

FIG. 3. The data and best-fit model predictions for the excess relative risk (ERR) for incidence of specific tumor types as function of age at exposure for mice irradiated with 1.9 Gy. The model was fitted to data for all doses used (see next figure), not just to the points shown here.

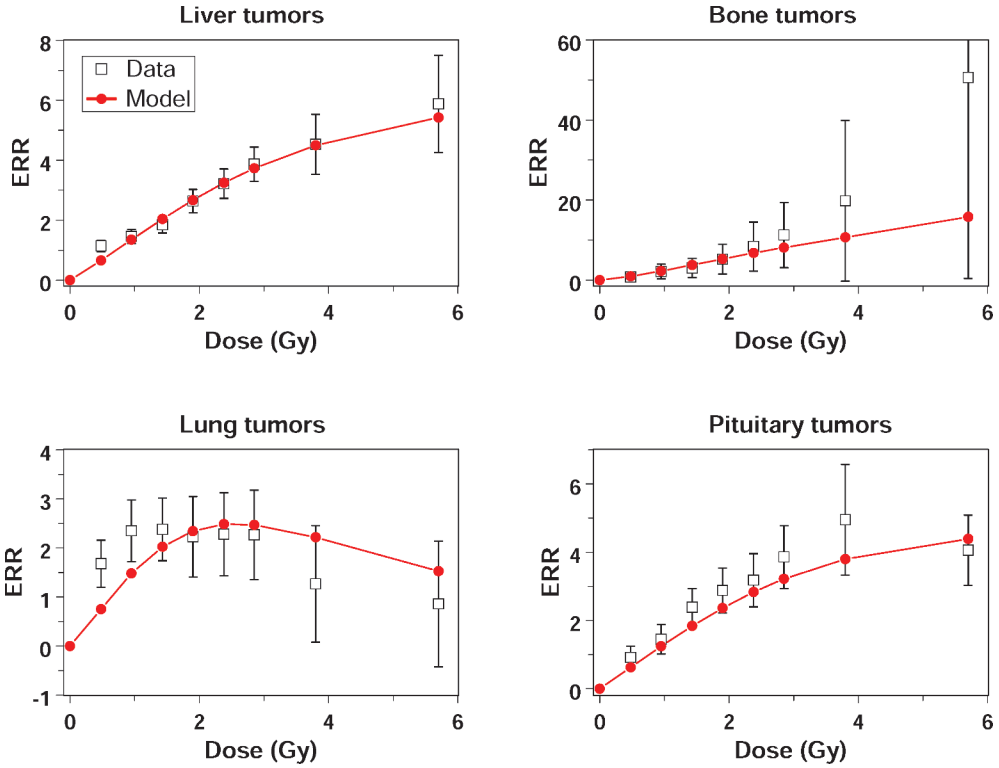

FIG. 4. The data and best-fit model predictions for the excess relative risk (ERR) for incidence of specific tumor types as function of dose for mice irradiated at age 0 days.

(not shown). However, the rapid increase in lung tumor ERR observed at relatively low doses (<1 Gy) could not be well reproduced by our model given the other data (i.e. an effective plateau of the ERR between 1 and 3 Gy). A possible explanation is that radiogenic lung tumor risk may be substantially affected by factors such as the bystander effect, which would tend to produce plateau-like dose–response shapes at low or moderate doses [e.g. refs. (*30–32*)] and has been postulated to be important for lung carcinogenesis by high-LET radiation [e.g. refs. (*33–35*)]. For bone tumors, the data may suggest a linear-quadratic rather than a linear dose–response shape.

An important goal of the present paper is to investigate the quantitative roles of different mechanisms, such as initiation and promotion, in the overall radiation-induced cancer risk. This can be done mathematically as follows:

Just after irradiation (i.e. $T_y = 0$), and assuming as we do here that $Z = 1$ and $\beta = 0$, the relative risk (RR) simplifies to

$$\mathrm{RR} = (1 + Y\,D)\exp[-\alpha\,D][b\,X\,D + \exp[b\,T_x] - 1]/(\exp[b\,T_x] - 1). \quad (3)$$

By setting either X or Y to zero, the RR can be decomposed into terms that contain only radiation-induced initiation ($\mathrm{RR_i}$), only radiation-induced promotion ($\mathrm{RR_p}$), and both initiation and promotion together ($\mathrm{RR_b}$):

$$\begin{aligned} \mathrm{RR_i} &= \exp[-\alpha\,D][b\,X\,D + \exp[b\,T_x] - 1]/(\exp[b\,T_x] - 1), \\ \mathrm{RR_p} &= (1 + Y\,D)\exp[-\alpha\,D], \\ \mathrm{RR_b} &= \exp[-\alpha\,D]\left[b\,X\,Y\,D^2 - \exp[b\,T_x] + 1\right]/(\exp[b\,T_x] - 1). \end{aligned} \quad (4)$$

The pure promotion term $\mathrm{RR_p}$ is simply the product of the cell survival probability, $\exp[-\alpha\,D]$, and the dose dependence of promotion, $1 + Y\,D$. The pure initiation term $\mathrm{RR_i}$ involves both cell killing effects and the number of pre-malignant cells/niches up to age at exposure. The term $\mathrm{RR_b}$, which represents interactions between initiation, promotion and cell killing, can be interpreted as radiation-induced promotion of previously radiation-initiated niches. This interpretation intuitively explains the quadratic dose dependence of the term, considering the linear individual dependences of initiation and promotion.

The behavior of Eq. (4) was investigated using the best-fit parameter values for different tumor types. It is shown using mouse liver tumors as an example in Fig. 5. The figure graphically illustrates the model property that the initiation-dependent terms $\mathrm{RR_i}$ and $\mathrm{RR_b}$ decline with age at exposure (panels A, C), for reasons described earlier, whereas the promotion-only term $\mathrm{RR_p}$ is independent of age at exposure, because for a single acute dose the model analyzes promotion as simply a multiplicative amplification of the number of pre-malignant cells. However, when expressed as a percentage of total RR, the pure initiation contribution $\mathrm{RR_i/RR}$ is constant with age at exposure (panels B, D). It is also notable that the contributions of initiation, promotion, initiation-promotion interactions, and cell killing are also dose-dependent, as Fig. 5 clearly demonstrates.

The negative values for initiation-promotion interactions ($\mathrm{RR_b}$) seen at older ages at exposure are, in a sense, a mathematical artifact of the definition of RR. This can be clearly seen from the structure of Eq. (4). For example, assume there is no radiation exposure, so $D = 0$. Then $\mathrm{RR_i} = 1$, $\mathrm{RR_p} = 1$, and $\mathrm{RR_b} = -1$, so total RR, which is the sum of all three terms, equals unity, as intuitively expected. As radiation dose increases, all three terms are increased, making $\mathrm{RR} > 1$, but $\mathrm{RR_b}$ can still be < 0 at sufficiently old ages at exposure (T_x).

DISCUSSION

Here we presented an analysis of radiation-induced mouse carcinogenesis using a data set well suited to investigate the dependences of cancer risk on age at exposure and time since exposure. The biologically based mathematical model we developed earlier (*16, 17*), which integrates the relatively short-term processes during irradiation and tissue recovery with more long-term processes that determine pre-malignant cell dynamics throughout the entire lifetime, is able to adequately describe these data, using a limited number of biologically plausible parameter values.

The best-fit model parameters generated by this analysis are of course mouse-specific and cannot be applied to humans because of life-span differences and other factors. However, our results suggest that the general patterns of radiation carcinogenesis may be relatively similar for mice and humans, at least for the cancer types analyzed. Some conclusions drawn from analyzing the mouse data sets selected here, and which can have some importance for human risk estimation and carcinogenesis mechanisms, are presented below:

1. At young ages at exposure, the model suggests that mouse ERR is dominated by radiogenic initiation, whereas at older ages promotion becomes more important. Similar conclusions have been reported earlier by authors using the two-stage clonal expansion (TSCE) model on data from human atomic bomb survivors (*9, 36*). This implies that humans exposed to radiation as children are at risk mainly due to generation of new pre-malignant cells from normal ones by radiation-induced mutagenesis (i.e. initiation), whereas individuals exposed in adulthood are at

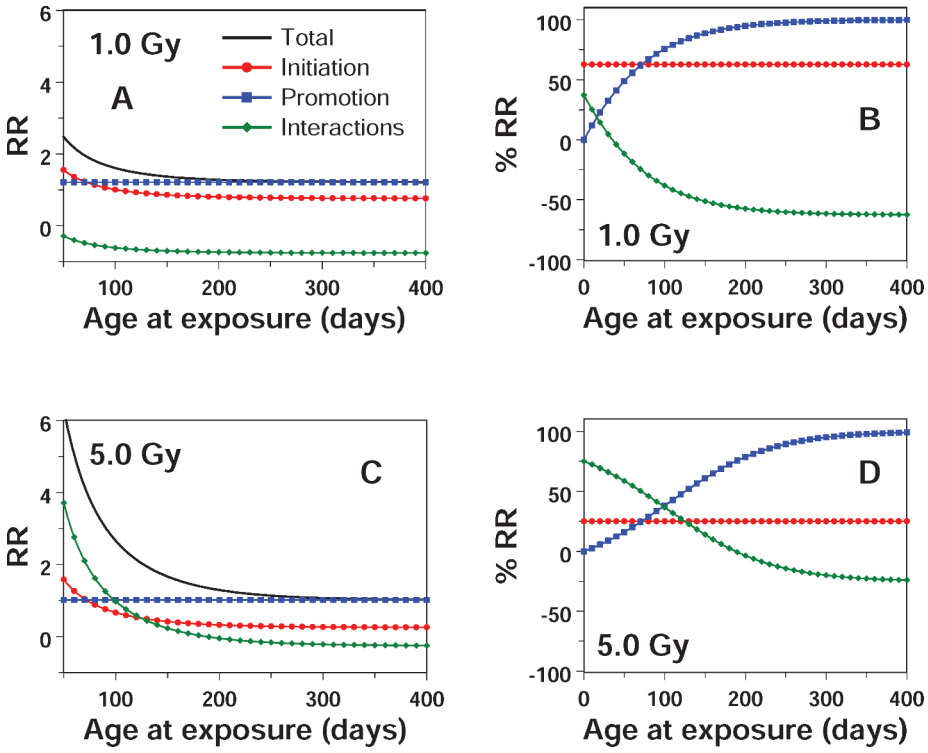

FIG. 5. Contributions of initiation, promotion and initiation-promotion interactions (i.e. promotion of radiation-initiated pre-malignant cells), all influenced by cell killing, to predicted liver tumor relative risk (RR) just after irradiation. Panel A shows total RR and its components for a dose of 1 Gy, and panel B shows the percentage contributions of these components as a function of age at exposure. Panels C and D show the same analysis at a dose of 5 Gy. Best-fit parameter values from Table 2 were used. In Panels A and C the *x* axis starts at 50 days because for younger ages at exposure the predicted RR is too large to conveniently show on the same vertical scale with the RR at older ages at exposure, and a logarithmic vertical scale is not possible because of negative values.

risk mainly due to radiation-induced increases in the sizes of already existing pre-malignant cell clones (i.e. promotion). Non-targeted radiation effects mediated by intercellular signaling may be involved in both initiation and promotion.

2. For exposure at very young ages, around the time of birth, mouse cancer risks are actually lower than at somewhat older ages, corresponding to childhood (*21, 22*). This finding is supported by recent analyses of human atomic bomb survivors irradiated *in utero* (*29*) and suggests that irradiation of the fetus and neonate may not be as dangerous in terms of cancer risk as previously thought. As noted earlier, our model in its current form does not predict this trend adequately. Further model development is needed to address this issue.
3. The mouse ERR tends to decrease with both age at exposure and time since exposure. The oldest age at exposure was 1 year, which is about one-third of the maximum life span of the mice studied and thus roughly corresponds to mid adulthood in humans. Similar trends have also been found in atomic bomb survivors, e.g. (*9, 36–39*). Some recent data analyses, which focus more attention on the older age-at-exposure subgroups of atomic bomb survivors (*39–42*), suggest that the radiation-related ERR for cancer induction decreases with age at exposure only until exposure ages of 30 to 40, while for older ages at exposure the ERR may not decrease further and, for many cancer sites (as well as for all cancers combined), the ERR may actually increase, generating "U-shaped" age-at-exposure dependences. If true, these findings can have significant societal implications where radiation exposure of adults is involved, for example for occupational radiation exposure limits and for new CT-based screening modalities of asymptomatic adults. Our formalism can describe either a decreasing or an increasing ERR trend at older ages at exposure, depending on parameter values, and is therefore potentially useful for analyzing data sets with both types of ERR patterns. According to the model, promotion-related ERR can increase as a function of age at exposure if the parameter for homeostatic regulation of the number of pre-malignant stem cells per niche (δ) is greater than zero. "U-shaped" age-at-exposure patterns for the ERR and for excess lifetime risk can therefore be generated by the model, where the initial decline is

dominated by initiation and the subsequent increase is dominated by promotional effects (Shuryak *et al.*, submitted for publication).

In conclusion, mechanistic analysis of animal and human data, using biologically motivated formalisms that model both initiation and promotion on both a short and a long time scale, may enhance the understanding of radiation-induced carcinogenesis. Our findings are consistent with the hypothesis that the general mechanistic patterns of radiation carcinogenesis may be relatively similar for mice and humans but that the balance between initiation and promotion may vary considerably among different cancer types.

ACKNOWLEDGMENTS

This work was supported through NIAID grant U19-AI67773 and NASA grant NSCOR04-0014-0017/NNJ04HJ12G/NNJ06HA28G.

Received: January 16, 2010; accepted: May 21, 2010; published online: July 14, 2010

REFERENCES

1. R. K. Sachs and D. J. Brenner, Solid tumor risks after high doses of ionizing radiation. *Proc. Natl. Acad. Sci. USA* **102**, 13040–13045 (2005).
2. R. K. Sachs, I. Shuryak, D. Brenner, H. Fakir, L. Hlatky and P. Hahnfeldt, Second cancers after fractionated radiotherapy: Stochastic population dynamics effects. *J. Theor. Biol*. **249**, 518–531 (2007).
3. I. Shuryak, R. K. Sachs, L. Hlatky, M. P. Little, P. Hahnfeldt and D. J. Brenner, Radiation-induced leukemia at doses relevant to radiation therapy: modeling mechanisms and estimating risks. *J. Natl. Cancer Inst*. **98**, 1794–1806 (2006).
4. A. C. Upton, The state of the art in the 1990's: NCRP Report No. 136 on the scientific bases for linearity in the dose–response relationship for ionizing radiation. *Health Phys*. **85**, 15–22 (2003).
5. K. A. Lindsay, E. G. Wheldon, C. Deehan and T. E. Wheldon, Radiation carcinogenesis modelling for risk of treatment-related second tumours following radiotherapy. *Br. J. Radiol*. **74**, 529–536 (2001).
6. S. B. Curtis, W. D. Hazelton, E. G. Luebeck and S. H. Moolgavkar, From mechanisms to risk estimation—bridging the chasm. *Adv. Space Res*. **34**, 1404–1409 (2004).
7. E. G. Luebeck and W. D. Hazelton, Multistage carcinogenesis and radiation. *J. Radiol. Prot*. **22**, A43–A49 (2002).
8. R. K. Sachs, M. Chan, L. Hlatky and P. Hahnfeldt, Modeling intercellular interactions during carcinogenesis. *Radiat. Res*. **164**, 324–331 (2005).
9. W. F. Heidenreich, H. M. Cullings, S. Funamoto and H. G. Paretzke, Promoting action of radiation in the atomic bomb survivor carcinogenesis data? *Radiat. Res*. **168**, 750–756 (2007).
10. W. F. Heidenreich, L. Tomasek, A. Rogel, D. Laurier and M. Tirmarche, Studies of radon-exposed miner cohorts using a biologically based model: comparison of current Czech and French data with historic data from China and Colorado. *Radiat. Environ. Biophys*. **43**, 247–256 (2004).
11. P. Armitage, Multistage models of carcinogenesis. *Environ. Health Perspect*. **63**, 195–201 (1985).
12. P. Armitage and R. Doll, The age distribution of cancer and a multi-stage theory of carcinogenesis. *Br J. Cancer* **VIII**, 1–12 (1954).
13. S. Moolgavkar, Multistage models for carcinogenesis. *J. Natl. Cancer Inst*. **65**, 215–216 (1980).
14. S. H. Moolgavkar, The multistage theory of carcinogenesis and the age distribution of cancer in man. *J. Natl. Cancer Inst*. **61**, 49–52 (1978).
15. S. H. Moolgavkar and E. G. Luebeck, Multistage carcinogenesis and the incidence of human cancer. *Genes Chromosomes Cancer* **38**, 302–306 (2003).
16. I. Shuryak, P. Hahnfeldt, L. Hlatky, R. K. Sachs and D. J. Brenner, A new view of radiation-induced cancer: integrating short- and long-term processes. Part I: approach. *Radiat. Environ. Biophys*. **48**, 263–274 (2009).
17. I. Shuryak, P. Hahnfeldt, L. Hlatky, R. K. Sachs and D. J. Brenner, A new view of radiation-induced cancer: integrating short- and long-term processes. Part II: second cancer risk estimation. *Radiat. Environ. Biophys*. **48**, 275–286 (2009).
18. W. F. Heidenreich and R. Hoogenveen, Limits of applicability for the deterministic approximation of the two-step clonal expansion model. *Risk Anal*. **21**, 103–105 (2001).
19. G. A. Colditz and B. A. Rosner, What can be learnt from models of incidence rates? *Breast Cancer Res*. **8**, 208 (2006).
20. G. A. Colditz and A. L. Frazier, Models of breast cancer show that risk is set by events of early life: prevention efforts must shift focus. *Cancer Epidemiol. Biomarkers Pres*. **4**, 567–571 (1995).
21. S. Sasaki and N. Fukuda, Dose–response relationship for induction of solid tumors in female B6C3F1 mice irradiated neonatally with a single dose of gamma rays. *J. Radiat. Res. (Tokyo)* **40**, 229–241 (1999).
22. S. Sasaki and N. Fukuda, Temporal variation of excess mortality rate from solid tumors in mice irradiated at various ages with gamma rays. *J. Radiat. Res. (Tokyo)* **46**, 1–19 (2005).
23. R. L. Ullrich, Tumor induction in BALB/c female mice after fission neutron or gamma irradiation. *Radiat. Res*. **93**, 506–515 (1983).
24. E. I. Azzam, S. M. de Toledo and J. B. Little, Oxidative metabolism, gap junctions and the ionizing radiation-induced bystander effect. *Oncogene* **22**, 7050–7057 (2003).
25. P. Dent, A. Yacoub, J. Contessa, R. Caron, G. Amorino, K. Valerie, M. P. Hagan, S. Grant and R. Schmidt-Ullrich, Stress and radiation-induced activation of multiple intracellular signaling pathways. *Radiat. Res*. **159**, 283–300 (2003).
26. R. Mikkelsen, Redox signaling mechanisms and radiation-induced bystander effects. *Hum. Exp. Toxicol*. **23**, 75–79 (2004).
27. A. Oriya, K. Takahashi, O. Inanami, T. Miura, Y. Abe, M. Kuwabara and I. Kashiwakura, Individual differences in the radiosensitivity of hematopoietic progenitor cells detected in steady-state human peripheral blood. *J. Radiat. Res. (Tokyo)* **49**, 113–121 (2008).
28. T. M. Phillips, W. H. McBride and F. Pajonk, The response of $CD24^{-/low}/CD44^{+}$ breast cancer-initiating cells to radiation. *J. Natl. Cancer Inst*. **98**, 1777–1785 (2006).
29. D. L. Preston, H. Cullings, A. Suyama, S. Funamoto, N. Nishi, M. Soda, K. Mabuchi, K. Kodama, F. Kasagi and R. E. Shore, Solid cancer incidence in atomic bomb survivors exposed in utero or as young children. *J. Natl. Cancer Inst*. **100**, 428–436 (2008).
30. E. J. Hall, The bystander effect. *Health Phys*. **85**, 31–35 (2003).
31. O. V. Belyakov, S. A. Mitchell, D. Parikh, G. Randers-Pehrson, S. A. Marino, S. A. Amundson, C. R. Geard and D. J. Brenner, Biological effects in unirradiated human tissue induced by radiation damage up to 1 mm away. *Proc. Natl. Acad. Sci. USA* **102**, 14203–14208 (2005).
32. G. Schettino, M. Folkard, K. M. Prise, B. Vojnovic, K. D. Held and B. D. Michael, Low-dose studies of bystander cell killing with targeted soft X rays. *Radiat. Res*. **160**, 505–511 (2003).
33. D. J. Brenner and R. K. Sachs, Do low dose-rate bystander effects influence domestic radon risks? *Int. J. Radiat. Biol*. **78**, 593–604 (2002).
34. D. J. Brenner and R. K. Sachs, Domestic radon risks may be dominated by bystander effects—but the risks are unlikely to be greater than we thought. *Health Phys*. **85**, 103–108 (2003).

35. S. B. Curtis, E. G. Luebeck, W. D. Hazelton and S. H. Moolgavkar, The role of promotion in carcinogenesis from protracted high-LET exposure. *Phys. Med.* **17** (Suppl. 1), 157–160 (2001).

36. W. F. Heidenreich, E. G. Luebeck, W. D. Hazelton, H. G. Paretzke and S. H. Moolgavkar, Multistage models and the incidence of cancer in the cohort of atomic bomb survivors. *Radiat. Res*. **158**, 607–614 (2002).

37. D. A. Pierce and M. L. Mendelsohn, A model for radiation-related cancer suggested by atomic bomb survivor data. *Radiat. Res*. **152**, 642–654 (1999).

38. D. A. Pierce and M. Vaeth, Age–time patterns of cancer to be anticipated from exposure to general mutagens. *Biostatistics* **4**, 231–248 (2003).

39. D. L. Preston, E. Ron, S. Tokuoka, S. Funamoto, N. Nishi, M. Soda, K. Mabuchi and K. Kodama, Solid cancer incidence in atomic bomb survivors: 1958–1998. *Radiat. Res*. **168**, 1–64 (2007).

40. National Research Council, Committee to Assess Health Risks from Exposure to Low Levels of Ionizing Radiation, *Health Risks from Exposure to Low Levels of Ionizing Radiation: BEIR VII Phase 2*. The National Academic Press, Washington, DC, 2005.

41. M. P. Little, Heterogeneity of variation of relative risk by age at exposure in the Japanese atomic bomb survivors. *Radiat. Environ. Biophys*. **48**, 253–262 (2009).

42. L. Walsh, Heterogeneity of variation of relative risk by age at exposure in the Japanese atomic bomb survivors. *Radiat. Environ. Biophys*. **48**, 345–347 (2009).